AGU PUBLICATIONS

Water Resources Research

RESEARCH ARTICLE

10.1002/2014WR016802

Seeing the landscape for the trees: Metrics to guide riparian shade management in river catchments

Matthew F. Johnson[1] and Robert L. Wilby[2]

[1]School of Geography, University of Nottingham, Nottingham, UK, [2]Department of Geography, Loughborough University, Leicestershire, UK

Key Points:

- Temperature over long stretches of river will not be affected by riparian shade
- Midreaches of headwater streams are most responsive to riparian shade
- To offset a 1°C temperature rise, 1 km of trees is necessary in UK small streams

Correspondence to:
M. F. Johnson,
M.Johnson@nottingham.ac.uk

Citation:
Johnson, M. F., and R. L. Wilby (2015), Seeing the landscape for the trees: Metrics to guide riparian shade management in river catchments, *Water Resour. Res.*, *51*, 3754–3769, doi:10.1002/2014WR016802.

Received 14 DEC 2014
Accepted 2 MAY 2015
Accepted article online 6 MAY 2015
Published online 27 MAY 2015

Abstract Rising water temperature (Tw) due to anthropogenic climate change may have serious consequences for river ecosystems. Conservation and/or expansion of riparian shade could counter warming and buy time for ecosystems to adapt. However, sensitivity of river reaches to direct solar radiation is highly heterogeneous in space and time, so benefits of shading are also expected to be site specific. We use a network of high-resolution temperature measurements from two upland rivers in the UK, in conjunction with topographic shade modeling, to assess the relative significance of landscape and riparian shade to the thermal behavior of river reaches. Trees occupy 7% of the study catchments (comparable with the UK national average) yet shade covers 52% of the area and is concentrated along river corridors. Riparian shade is most beneficial for managing Tw at distances 5–20 km downstream from the source of the rivers where discharge is modest, flow is dominated by near-surface hydrological pathways, there is a wide floodplain with little landscape shade, and where cumulative solar exposure times are sufficient to affect Tw. For the rivers studied, we find that approximately 0.5 km of complete shade is necessary to off-set Tw by 1°C during July (the month with peak Tw) at a headwater site; whereas 1.1 km of shade is required 25 km downstream. Further research is needed to assess the integrated effect of future changes in air temperature, sunshine duration, direct solar radiation, and downward diffuse radiation on Tw to help tree planting schemes achieve intended outcomes.

1. Introduction

Water temperature (Tw) is critical to the survival, growth, and development of poikilothermic fauna such as fish and invertebrates [*Thackeray et al.*, 2010; *Martins et al.*, 2011; *Dallas and Rivers-Moore*, 2012; *Everall et al.*, 2015]. Global and regional assessments suggest that river Tw is rising due to climate change [*Isaak et al.*, 2010; *van Vleit et al.*, 2011; *Orr et al.*, 2015a]. Changes to catchment land use and hydrology, including the removal of riparian vegetation that shades channels from solar radiation, can also elevate Tw [*Rutherford et al.*, 2004; *Richardson and Béraud*, 2014]. Riparian vegetation has many impacts on waterways and, as a result, riparian buffer strips have long been a focus of river management and restoration [e.g., *Osborne and Kovacic*, 1993; *Everall et al.*, 2012; *Wilby et al.*, 2010; *Sweeney and Newbold*, 2014].

The thermal impact of riparian vegetation is widely recognized by the forestry sector in North America [see *Moore et al.*, 2005] and is attracting attention in the UK as a possible climate adaptation option [e.g., *Nisbet et al.*, 2011; *Environment Agency*, 2012]. Tree canopies increase long-wave radiation reaching the forest floor, but this only partially offsets substantial reductions in short-wave solar radiation, which may be 80% less than in open areas [e.g., *Davies-Colley et al.*, 2000]. A meta-analysis by *Bowler et al.* [2012] found that rivers with riparian trees had lower mean and maximum Tw than those without trees. Experimental work involving artificial shading of rivers also demonstrates the potential significance of shade in reducing Tw [*Johnson*, 2003]. Ultimately, daily and seasonal solar energy receipts depend on orbital variations and latitude.

Energy balance studies reveal that short-wave solar radiation is the major heat component of rivers, with other sources (including long-wave radiation, sensible, and latent heat transfers and frictional effects) being relatively minor [*Evans et al.*, 1998]. River discharge indirectly affects Tw by controlling water surface area available for energy exchanges; river flow velocity controls the length of time water is exposed to energy exchanges; and water volume determines heat capacity and thermal inertia [*Moore et al.*, 2005]. Other properties, such as suspended sediment load also affects the energy balance of the water column. Hence, moving downstream, rivers tend to be increasingly buffered against Tw change as discharge increases and the drainage network is progressively decoupled from the surrounding landscape.

Sensitivity of rivers to solar energy inputs may be further moderated by mixing of water of differing temperature, for example, from groundwater sources or tributaries [*Story et al*., 2003]. The base flow index provides a useful proxy for groundwater flow and was found to be a significant factor reducing maximum stream temperatures in the Columbia River basin [*Chang and Psaris*, 2013]. Projected changes in river flow regimes under climate change also have the potential to indirectly affect Tw by modifying the relative dominance of different hydrological pathways and flow volumes. For example, under a warming scenario, transition from a snowmelt dominated to pluvial regime would be expected to diminish influxes of cool meltwater in spring and cause more severe low flows in summer [*Mantua et al*., 2010; *Null et al*., 2013; *Ficklin et al*., 2014]. In turn, decreased spring/summer flows and rising stream temperatures reduce dissolved oxygen concentrations and sediment transport in snowmelt-dominated systems [*Ficklin et al*., 2013].

Daily mean and maximum Tw can be predicted from air temperature (Ta) using logistic regression analysis [e.g., *Kelleher et al*., 2012; *Chang and Psaris*, 2013; *Johnson et al*., 2014]. The relationship between Ta and Tw is not causal but is informative because of the high explanatory power of regressions (typically $r^2 > 0.8$) and availability of long-term, high-resolution Ta records. Moreover, logistic regression parameters can be used to infer controls of thermal sensitivity. For example, *Johnson et al*. [2014] found that the gradient of regressions was significantly correlated with cumulative upstream shade and groundwater inputs. Similarly, *Chang and Psaris* [2013] report that stream order and forest cover controlled regression parameters. In contrast, systematic measurement of all components of Tw heat budgets can be prohibitively expensive and logistically complex to collect over large numbers of sites or for extended field campaigns.

The effects of thermal inertia (due to water volume) and impact of advected heat from upstream, can be explored using coupled energy-hydrological models running at high spatial and temporal resolutions [e.g., *Cole and Wells*, 2002; *Chapra et al*., 2008]. Such models typically depend on extensive data inputs and processing times even for small areas. Here, the aim is to derive robust metrics to identify reaches where increased riparian shade might counter rising Tw given data that are widely available and/or inexpensive to collect. In order to achieve this outcome, we have the following research questions in mind. (1) What is the relative amount of tree and landscape shade over the surface drainage network in our study catchments? (2) What temporal and spatial factors govern thermal inertia and heat advection with distance downstream? (3) Where and by how much should riparian shade be increased to offset a unit rise in summer maximum Tw under climate change?

First, we combine landscape analysis in ArcGIS with Tw records for the River Dove and Manifold catchments, English Peak District to quantify; (i) the extent and distribution of tree cover, (ii) the relative significance of landscape and tree shade in reducing solar energy inputs to the river network, and (iii) the sensitivity of river reaches to shading. Second, the location of trees and their significance in the context of rising Tw was assessed by considering variations in river heat capacity. Third, logistic regression parameters derived from long-term Tw monitoring were used to interpret sensitivity of sites to future climate change. Finally, the implications of the study are discussed for other catchment types in order to inform planting schemes and Tw management more generally.

2. Methods

2.1. LUTEN Site Location and Field Surveys

The Loughborough University TEmperature Network (LUTEN) has been described previously by *Toone et al*. [2011], *Johnson et al*. [2014], and *Wilby et al*. [2014]. LUTEN is an array of 37 paired Ta-Tw monitoring sites along the Rivers Dove and Manifold, English Peak District (Figure 1). The catchments are located in an upland region (450 m above sea level), with an altitudinal range over the monitored reaches of 150 m. Both catchments receive over 1000 mm/yr rainfall and have annual average Ta = 8.9°C at site D10 (for the years 2010–2013). Land use is mainly cattle-grazed pasture. The Manifold is underlain by Millstone Grit whereas the Dove comprises a Millstone Grit-Carboniferous Limestone transition (Figure 1). The area of the Dove catchment is 83 km^2, and the Manifold is 64 km^2 upstream of the most downstream monitoring site in each case. Both river morphologies develop from narrow, incised channels in the headwaters to wider channels

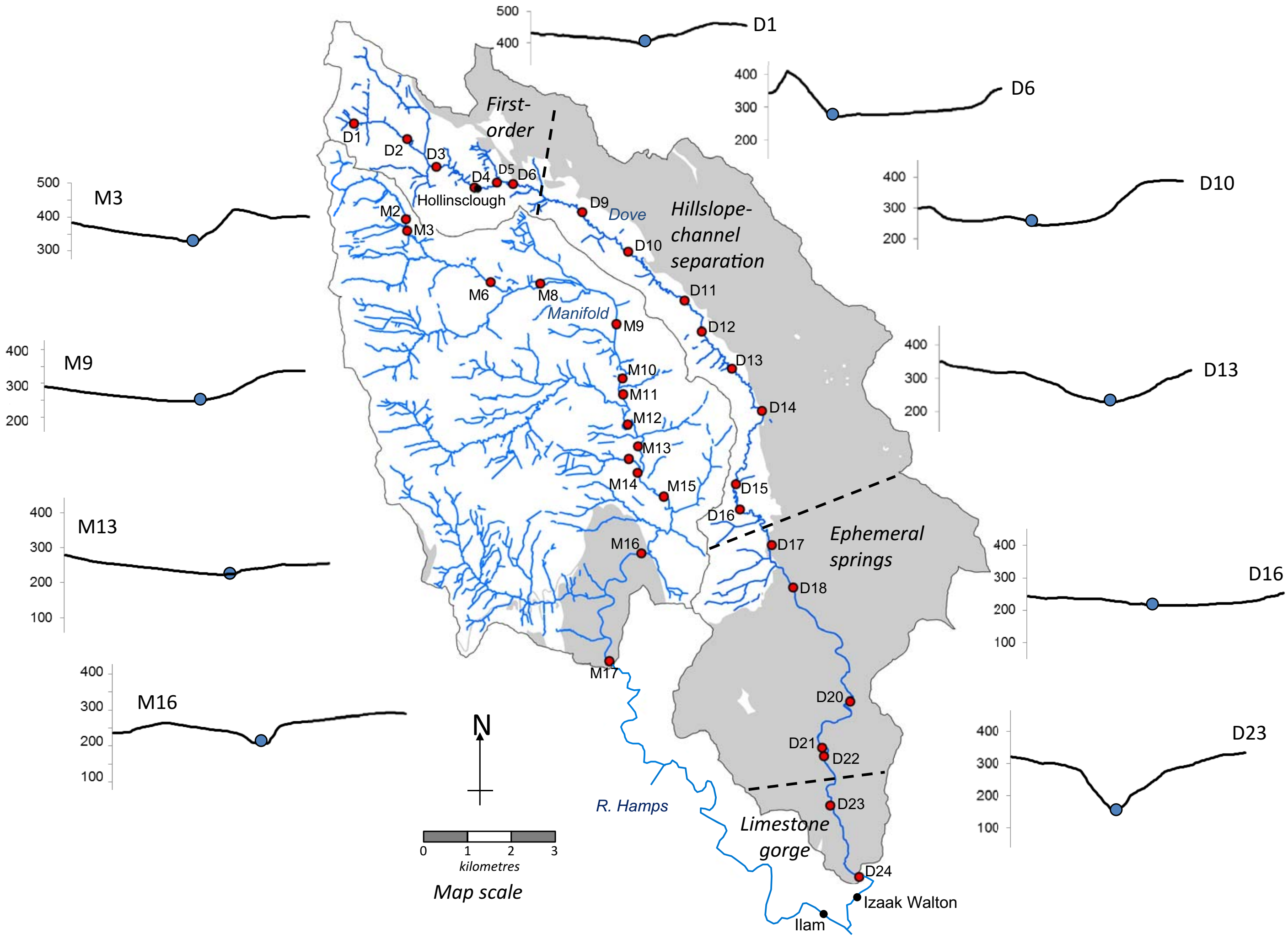

Figure 1. LUTEN sites in the Dove and Manifold catchments, English Peak District. Red points are monitoring sites; gray-shading indicates Limestone geology; white areas are Millstone Grit. Illustrative cross-sectional profiles are indicated for the Manifold (left) and Dove (right). Each cross-sectional profile is 3 km across with vertical scale in meters.

flowing through a broad floodplain. Lower reaches of the Dove eventually intersect Limestone and flows through a deep gorge (Figure 1). Tw at sites D16 to D24 are further affected by ~100 small weirs.

The River Dove has complex hydrogeology and is sustained by substantial groundwater inputs [*Edmunds*, 1971; *Abesser and Smedley*, 2008]. Eight distinct springs flow intermittently between D6 and D16. Four surface springs and large subsurface inputs of groundwater occur seasonally between sites D16 and D22. Eleven surface springs contribute groundwater to the main channel year-round between D22 and D24. Seasonal spot measurements were made of Tw and conductivity in surface springs and the main river channel but more frequently through Dovedale. Conductivity is higher in spring water and can be used as a marker to assess the relative contribution of spring water to main channel flows [*Johnson et al.*, 2014]. Tw measures are recorded every 15 min in surface spring flows at Crowdecote and in Dovedale (Figure 1).

2.2. Shade and Irradiance Maps

ArcGIS 10.3 was used to construct a landscape model of the Dove and Manifold using a 2 m resolution Digital Elevation Model (DEM) with the river network, watershed boundary, monitoring sites, and groundwater spring locations georeferenced. LiDAR has been used to map shade elsewhere in the UK [e.g., *Greenberg et al.*, 2012], but such data are not available for the Dove and Manifold, so aerial photographs from 2003 were used to digitize individual trees and woodland areas. This is the most recent aerial imagery and represents a snap-shot in time. However, no major forestry operations have taken place since 2003, maps were ground validated at river monitoring sites and found to be consistent. In addition, tree cover at LUTEN sites was monitored over the course of the three year experiment, with minimal change observed. Synthetic shade maps were then generated from the footprint of observed tree cover for heights of 10, 20, and 30 m. These represent juvenile, adult, and mature Ash (*Fraxinus excelsior*), respectively—the dominant tree species in the study area.

Shade maps were produced using the solar radiation function of *Fu and Rich* [2002], which uses global standard solar geometry equations to calculate solar radiation receipt across a DEM, based on site latitude and longitude, date, time of day, and slope angle. Calculation resolution was set to 14 days with the visible sky (skysize) divided into 512 discrete solar regions, which was deemed sufficient for monthly, catchment-scale radiation maps [see *Fu and Rich*, 2002 for more details]. Only direct solar radiation was considered in our analysis and the simplifying assumption made that trees allow no light penetration through the canopy. In reality, some light would penetrate the foliage, depending on species, age, canopy structure, and season, so our evaluation of the potential impact of trees on river shade is an upper bound estimate. Shade and radiation maps were generated for surfaces with no trees, juvenile, adult, and mature trees for each month and year as a whole. Comparisons were made between the duration of shade and the amount of solar energy incident over the catchments and along the river network.

To estimate maximum solar radiation incident on the river channel at higher temporal resolutions (5 min) than for GIS layers covering the whole catchment (monthly), solar elevation angles (i.e., height of the sun above the horizon θ_e) and azimuth angles (i.e., compass direction φ_s) at any given time at site latitude (52° N) were calculated using the algorithm of *NOAA* [2014], which is a global function, based on solar geometry. The solar radiation incident on the Earth's atmosphere is known as the Solar Constant and approximates 1.353 kW m^{-2}. However, the amount of radiation reaching the Earth's surface varies due to two main factors. First is the reduction in the power as solar energy passes through the Earth's atmosphere due to absorption by air and dust, quantified using the global function:

$$I_A = 1.353\,x\,0.7^{(AM^{0.678})} \tag{1}$$

where I_A (W m^{-2}) is solar irradiance incident on a perpendicular surface, 1.353 is the solar constant, 0.7 represents the fact that 70% of solar radiation incident on the atmosphere reaches the Earth's surface, 0.678 is derived empirically from measured data, and AM is the "air mass," which is equal to:

$$AM = \frac{1}{\cos(\theta_z) + 0.50572(96.07995 - \theta_z)^{-1.6364}} \tag{2}$$

where θ_z is the Zenith Angle (which is the complimentary angle to θ_e). Second, when the angle of incidence (which is elevation angle, θ_e) is not 90° vertical, solar radiation is spread over a larger area, effectively diluting intensity. This effect is quantified as:

$$I_{AD} = I_A \sin\,\theta_e \tag{3}$$

where I_{AD} (W m^{-2}) is the solar irradiance on a horizontal surface. Note that this estimate does not account for cloud cover or water vapor in the atmosphere, both of which have substantial impacts on solar irradiance by casting shade and reducing solar energy receipt at the Earth's surface. The value of I_{AD} does not account for surface albedo (i.e., reflectance), nor for diffuse radiation. Consequently, equation (3) is the maximum possible amount of direct solar radiation striking a horizontal surface at a given latitude. The river surface was also considered to be horizontal at this resolution, so the effect of channel slope on radiation receipt was ignored. However, sensitivity testing using channel gradients in the Dove (maximum 2.3°, mean 0.4°) and the Manifold (maximum 1.0°, mean 0.5°) indicates that river slope adds locally no more than 4% to direct radiation receipt. At the catchment-scale, ArcGIS layer outputs do account for nonhorizontal slopes. To convert I_{AD} (W m^{-2}), calculated at 5 min resolution, into solar energy (J m^{-2}), I_{AD} was multiplied by 300 s.

2.3. River Discharge and Thermal Sensitivity Analysis

Metrics were derived for thermal inertia and advection to explore the sensitivity of sites to shade. Thermal inertia due to increasing water volume with distance downstream was estimated by standardizing at-a-site irradiance by upstream catchment area, a widely used surrogate for discharge [e.g., *Hannah et al.*, 2008] that is readily derived from the DEM. Heat advection was estimated by standardizing at-a-site irradiance by all radiation incident over the upstream river network. The heat capacity (*C*) of water (~4180 kg J°C) was then used to estimate the length of continuous shade required to change Tw by 1°C at the two sites on the Dove, coinciding with river flow gauges maintained by the Environment Agency of England and Wales (EA). These sites are Hollinsclough (D4, 4.1 km from source) and Izaak Walton (D24, 31.2 km from source). The gauges record discharge every 15 min through a fixed cross section. Volume of flow (product of channel width (*w* m), depth (*d* m), and length (*l* m)) at these sites was used to estimate the energy (*E* J) required to change Tw by 1°C as:

$$E=([w\times d\times l]\times 1000)\times C \tag{4}$$

where 1000 converts water volume (m^3) to mass (kg). The time (*T* s) taken to accumulate radiative energy (*E*) over the surface *w.l* was calculated from NOAA solar estimates and ArcGIS layer outputs as:

$$T=E/I_{AD} \tag{5}$$

The velocity of water (v m s^{-1}) at the gauge was then used to determine how far a parcel of water would flow in the time taken to reach *E*, as:

$$L=v\times T \tag{6}$$

indicating the length (*L* m) of tree cover required to shade a river from radiation that is equivalent to a 1°C change in Tw. Note, this lower bound estimate does not account for heat from other sources, diffuse, or reflected radiation or for the fraction of direct radiation that penetrates the tree canopy.

2.4. Regression Modeling and Parameter Analysis

Maximum, mean, and minimum Ta and Tw were monitored with Gemini Aquatic II Tinytag thermistors at each monitoring site (Figure 1). Tinytags have a quoted accuracy of 0.2°C, which has been confirmed in laboratory experiments [*Johnson and Wilby*, 2013]. Data were recorded at 15 min resolution and are available for 3 years at 20 sites, and 2 years at a further 17 sites (Figure 1). Daily maximum Tw at each site was modeled given daily maximum Ta using logistic regression models, following *Mohensi et al.* [1998]:

$$TW=\frac{\alpha}{\left(1+\exp^{\gamma(\beta-T\alpha)}\right)} \tag{7}$$

where α is the model asymptote, β is the Ta where the gradient is steepest, and γ is the gradient term. Regression models were constructed for all sites for each year, as well as for all years combined. Detailed analysis of LUTEN data reveals that regression models perform well ($r = 0.82$ to 0.97) even when calibrated and validated with data reflecting contrasting weather conditions [*Johnson et al.*, 2014; *Wilby et al.*, 2014]. Spatial variations in these regression parameters are reinterpreted below in the context of the shade and heat analyses.

3. Results

3.1. Location and Extent of Tree Cover

Trees cover 6.8% of the Dove and 7.5% of the Manifold catchment. Average patch size across both catchments is 681 m^2 (S.D = 4563 m^2) but 16% of patches consist of single trees. The largest unbroken patch size was 0.26 km^2, comprising of an Ash woodland running through Dovedale. Trees bound the main channel of the Dove and Manifold for 44% and 35% of their lengths (13.7 km and 7.0 km), respectively. Patches bordering the rivers are typically just a few trees deep.

3.2. Location and Extent of Shade

Adult trees reduce annual radiation receipt over 51% and 55% of the surface area of the Dove and Manifold catchments but 92% and 89% of the main channel length of Dove and Manifold, respectively (Table 1). Approximately 7% of the Dove and Manifold catchments receive less than half of the solar radiation that would accrue if there were no trees. However, landscape shade is concentrated along drainage lines with 32% of Dove river network and 22% of the Manifold receiving less than 50% (Figure 2). Landscape provides most shade in the headwaters with much less for downstream reaches once floodplain development

Table 1. Surface Area of Tree Canopy and Tree Shade in the Dove and Manifold Catchments

Catchment	Dove	Manifold
Surface area shaded by landscape (%)	50.7	54.7
Total area covered by tree canopy (km^2)	5.7	4.8
Fraction of area covered by tree canopy (%)	6.8	7.5
Number of discrete tree patches	6770	8630
Average patch size (km^2)	0.0008	0.0006
Standard deviation of area (km^2)	0.006	0.003
Total area shaded (10 m trees) (km^2)	37.4	40.3
Total area shaded (20 m trees) (km^2)	49.8	48.0
Total area shaded (30 m trees) (km^2)	63.1	56.3

begins. Treeless reaches of the Dove (between 5 and 25 km from source) receive nearly 100% of potential direct solar radiation. Equivalent distances on the Manifold are 9–17 km from source. Beyond 25 km along the Dove and 17 km along the Manifold, the Limestone gorge increases landscape shade, decreasing solar radiation receipt by 16% and 7%, respectively (Figure 3).

Solar radiation is greatest at midday in summer, when solar angles are high and solar azimuth is south (Figure 4). Over 69% of the total radiation received at 52° N is from solar angles greater than 30°, despite the fact that these angles occur only 37% of the time. Landscape shades all solar angles in the headwaters of the Dove and Manifold, but only relatively low solar angles at more downstream sites (Figure 5). Conversely, trees shade a similar range of angles to the landscape in the headwaters, but shade higher solar angles than the landscape downstream (Figure 5). Due to variations in solar radiation intensity, the proportion of time in shade exceeds the proportion of radiation reduced by shade (Figure 3).

Preferential shading at certain solar angles leads to seasonality in shade, and to differences in shade provided by trees and the landscape (Figure 3). The difference in radiation receipt between landscape only and landscape plus trees is less than 15% of the annual total irradiance across 73% of the catchment area. Most of this difference occurs in spring and summer, when solar angles, and therefore solar radiation, are greatest (at the latitude of the catchment) (Figure 2). In autumn and winter, the difference in shading between trees and the landscape is minimal, even when leaf fall is neglected.

In order to block, solar angles greater than 30° and thereby reduce the majority of solar irradiance requires trees to be sited near rivers (Figure 6). For example, a 10 m high tree casts 17.6 m of shade at 30° solar elevation angles, whereas at 60° angles (responsible for 23% of solar energy in the catchments) the shadow cast is 5.8 m long. Although a larger area is shaded in winter, when solar angles are lower, the benefit of shading is greatest in summer, when solar angles and intensities are highest. To put these values into context, the maximum channel widths of the Dove and Manifold are 14 and 12 m, respectively. The Dove is less than 6 m wide for the first 24 km from source, therefore requiring a single line of 10 m tall trees on each bank to shade the width of the river. The transition to partial shade is due to increased channel width as well as the north-south orientation of the river.

3.3. Sensitivity of River Reaches to Shading

Cumulative direct solar energy received by the drainage network increases with distance downstream (Figure 7a). A channel without trees, shaded only by the landscape receives substantially more radiation than reaches shaded by trees: each year treeless reaches of the Dove accumulate 1.54×10^6 MJ/km compared with 0.39×10^6 MJ/km when trees are present. This also means that more heat is advected from upstream when the landscape is treeless. Moreover, there are step changes in heat with distance downstream due to tributary inputs which for the Dove contribute 43% of the energy received by a network without trees and 41% with adult trees (Figure 7b). Tributaries contribute 88% of the energy received by the Manifold network both with and without adult trees. Standardizing annual energy received at a site by total cumulative upstream energy receipt reveals the significance of heat advection. After 50 m, local radiation adds less than 1% to the heat gained from upstream in the Dove network and less than 0.1% after 300 m (Figure 7c).

Catchment area increases from 2.1 km^2 at site D2 to 82.5 km^2 at site D24 at an average rate of ~3 km^2 per kilometer of river length in the Dove (Figure 8b) and 3.4 km^2 per kilometer in the Manifold (not shown). Heat capacity calculations suggest that to reduce Tw by 1°C at Hollinsclough (6.7 km from source) at midday on the solar equinox would require 0.5 km of adult tree cover. Under the same conditions, it would require 1.1 km of tree cover at Izaak Walton (31.2 km from source). Table 2 shows the length of riparian shade theoretically required to cool Tw by 1°C at midday on the 15th day of each month at the two gauging stations. We pay particular attention to June–July because this is the month during which maximum Tw is typically experienced in the Dove and Manifold [*Wilby et al.*, 2012].

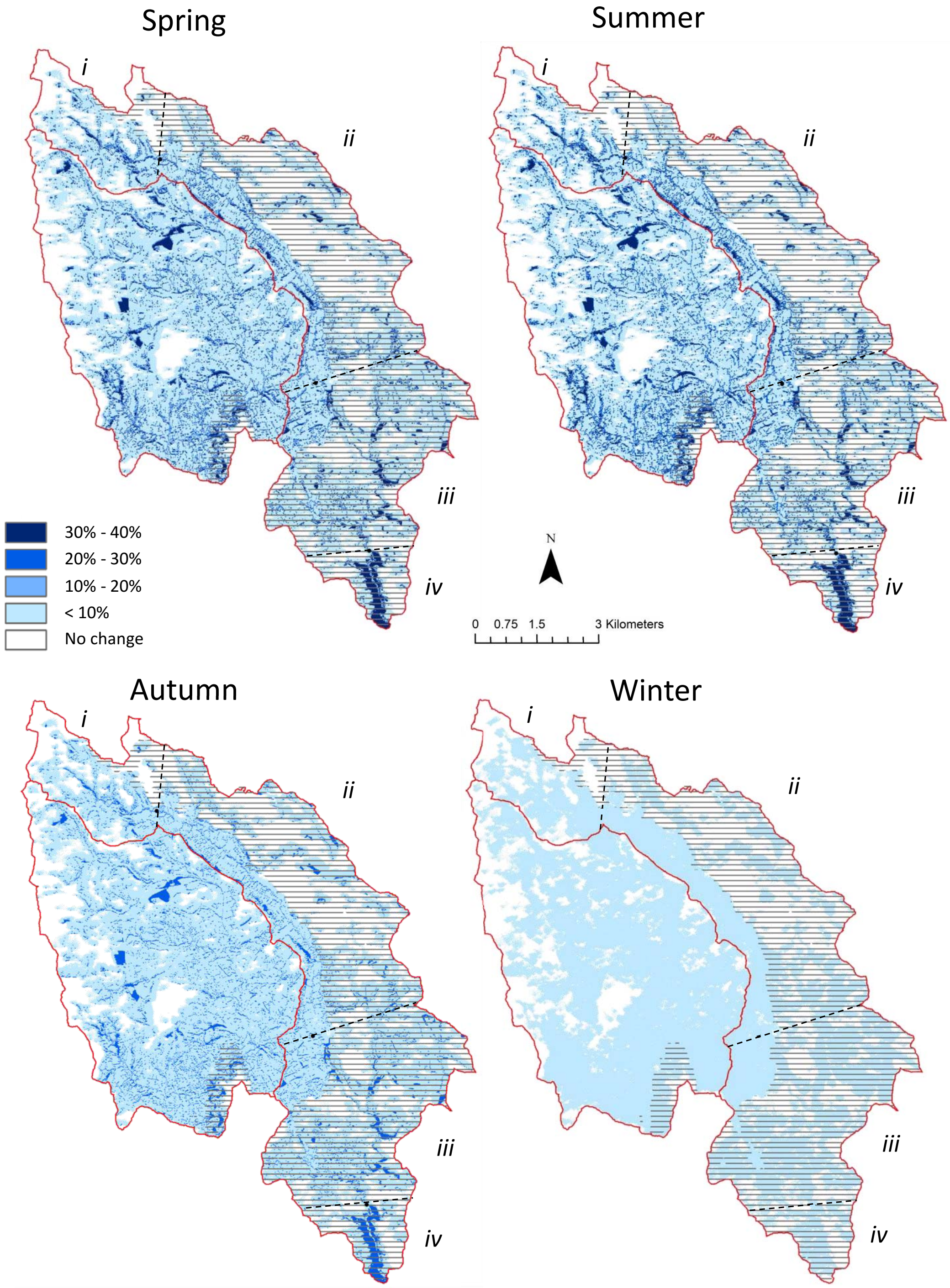

Figure 2. Difference in solar radiation receipt due to 30 m tall vegetation cover shown as a percentage of the potential annual total. Summer is June–August, Spring is March–May, Autumn is September–November, and Winter is December–February. White areas indicate no change. Horizontal hatching indicate area overlying limestone. Dashed lines indicate the four distinct hydrological regimes of the Dove; (i) first-order, (ii) hillslope-channel decoupling, (iii) ephemeral groundwater, and (iv) limestone gorge.

3.4. Logistic Regression Analysis

Logistic regression models describe the Ta-Tw relationship well at all LUTEN sites (the lowest r^2 value is still 0.86 at site D20 despite the substantial influence of groundwater). The three model parameters are: α which is the asymptote of the model, indicating the maximum predicted Tw due to evaporative cooling at high Ta; β which is the Ta where the gradient is greatest, and; γ which is the model gradient at β.

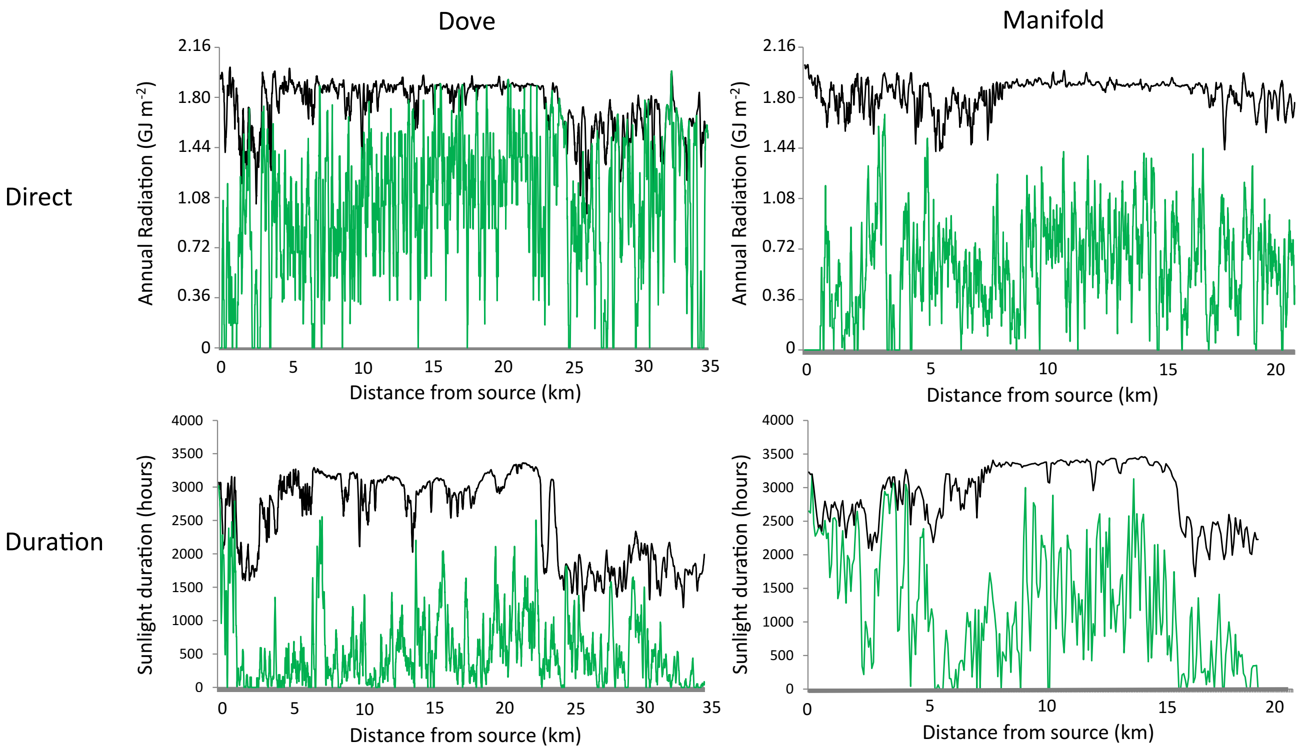

Figure 3. Downstream profiles of estimated annual direct solar radiation (Gigajoules) (upper panels) and time in shade (hours) (lower panels) for landscapes with trees (green) and without trees (black) in the Dove (left) and Manifold (right).

Values of α increase with distance downstream until D22 and drop off markedly at D23 (Figure 8d). For the first 19 km of the River Dove (D1 to D17), α increases by 0.5°C for every 1 km of downstream distance ($r^2 = 0.98$). At sites D20 and D22 (26 and 28 km), α remains at 24°C but is more variable between years than upstream sites (Figure 8d). Values of γ are highest in the headwater (D1 and D2) and decline with distance downstream to 19 km (D17) where they begin to increase. Regression model parameters vary between years according to weather conditions, but the general pattern remains the same (see Figure 8d).

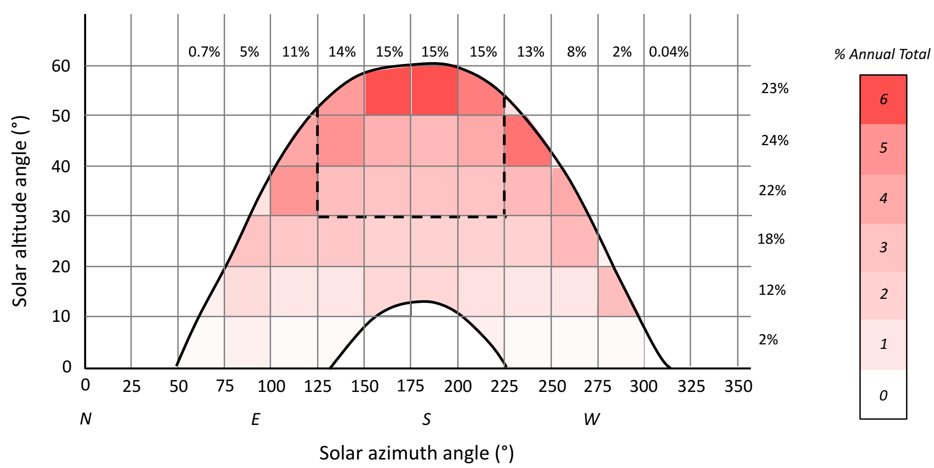

Figure 4. The elevation angle (e.g., angle of incidence) and azimuth angle (i.e., compass direction) of the sun over a year at 52° latitude. Shading indicates relative proportion of solar radiation occurring at that solar position over a year. Percentages of the total solar radiation budget at each azimuth or elevation angle are denoted.

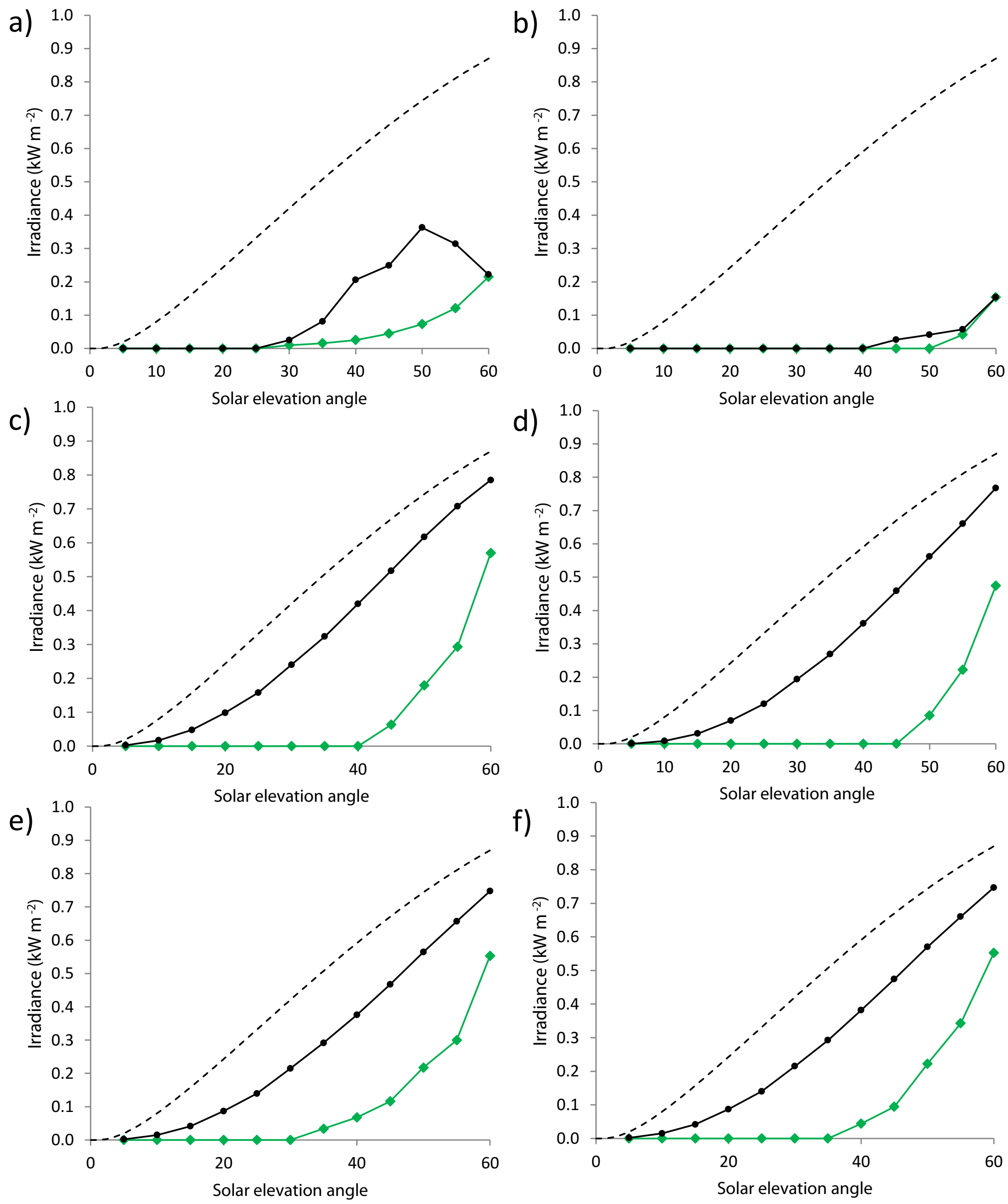

Figure 5. The irradiance (kW m^{-2}) incident at each solar elevation angle at site D2 (a,b), D10 (c,d), and D16 (e,f) on the River Dove for the rising sun (a,c,e) and setting sun (b,d,f). The black line indicates landscape shade and the green line is landscape plus 20 m high tree shade. The maximum possible radiation at each elevation angle is given by the dashed line.

Using conductivity as a marker for groundwater reveals that inputs are substantial in the headwaters and downstream where spring flows from the Limestone outcrop (Figure 8c). Continuous monitoring at three sites indicates groundwater annually averaged Tw is 9.1°C through Dovedale, with an annual range of 0.5°C (S.D = 0.04°C). Groundwater inputs have a substantial impact on thermal regime, and affect all logistic regression parameters [see *Johnson et al.*, 2014].

4. Discussion

4.1. River Reaches Most Sensitive to Tree Shade

Tree cover in the Dove and Manifold is broadly representative of the England average (8%) [*Forestry Commission*, 2003], but is less than parts of mainland Europe (37%) [*FAO*, 2010]. However, tree cover is

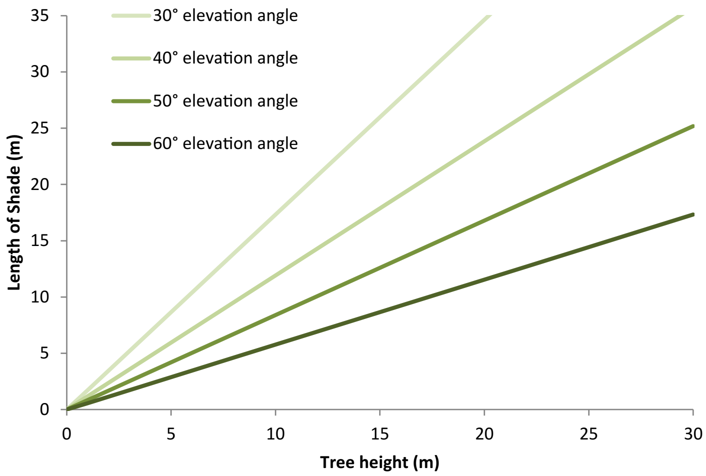

Figure 6. Length of shade cast by trees of selected height at solar elevation angles ranging from 30° to 60° from the horizon.

concentrated along river networks compared with the rest of the catchment. Trees on river banks shade high solar angles and, consequently, shade high magnitude irradiance. This shade is more heterogeneous than shadows at lower solar angles which are created by landscape and trees over the majority of the catchment. Even so, shading high solar angles is disproportionately significant for the river network because of the proximity of trees to the channel, resulting in 40% of the river network receiving less than 50% of the solar radiation that would be received if trees were absent.

Loss of tree cover, for example due to Ash dieback, could have dramatic consequences for Tw in the Dove and Manifold by increasing energy receipts by the river. However, tree shade is of least relative significance in the headwaters and in the gorge sections of Dovedale, because the landscape already provides shading, including at high solar angles. In headwaters (0–6 km from source) trees provide, on average, an additional 2000 min of shade, but reduce annual radiation receipt by 15% compared with a treeless landscape. At

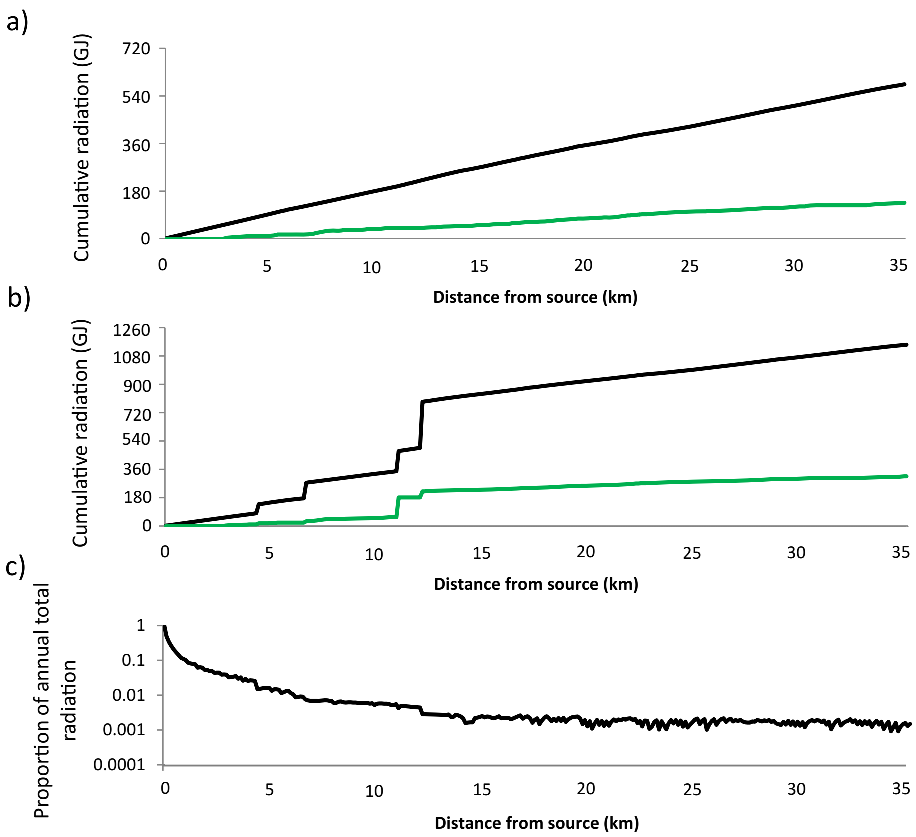

Figure 7. Estimated cumulative solar energy (GJ) receipt upstream of points on (a) the main channel of the River Dove and (b) for the whole Dove network taking into account the influence of tributaries (evidenced by step changes in the profile). The black line incorporates landscape shade and the green line is landscape plus 30 m tree shade. (c) Solar energy receipt "at-a-site" as a proportion of the aggregate receipt across the upstream network.

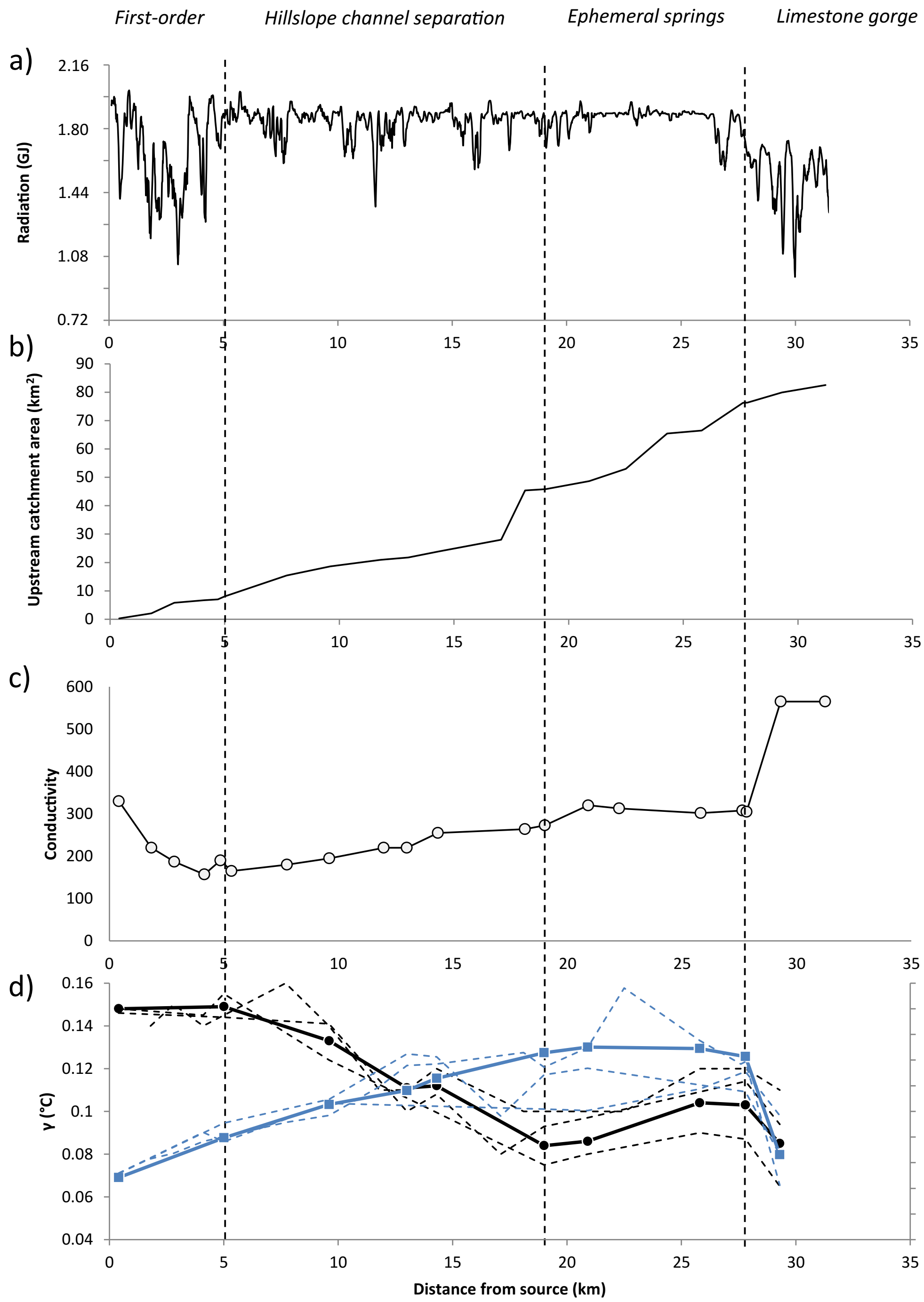

Figure 8. (a) Radiation receipt with distance from source in the River Dove without trees; (b) upstream catchment area of the Dove; (c) conductivity of water in the main channel of the River Dove; (d) the asymptote (α; blue) and gradient (γ; black) term of logistic regression models constructed on daily maximum Ta and Tw data from March 2011 to February 2013 (thick lines) and values for individual years (dashed lines).

intermediate reaches (6–20 km from source), with floodplain, the landscape provides little shade at high solar angles, resulting in the river receiving nearly 100% of the potential solar radiation. In these locations, tree cover would reduce radiation receipts by 25%.

4.2. Relative Significance of Shade in Context of River Regime

While tree cover and radiation maps show spatial variations in riparian shade, they do not indicate which river reaches might benefit most from increased canopy cover. Thermal inertia and advected heat from

Table 2. Estimated Length of Continuous 20 m High Tree Shade Required to Change Tw by 1°C at 11 A.M. on the 15th Day of Each Month[a]

		Discharge (m^3)	Heat Capacity (kg J°C)	Time to Reach Capacity (s)	Average Velocity ($m\ s^{-1}$)	Required Shade (km)
D4	January	0.42	1,328,166	9,600	0.67	6.4
	February	0.36	1,188,790	4,200	0.63	2.7
	March	0.33	1,110,618	2,700	0.62	1.7
	April	0.25	908,214	1,800	0.57	1.0
	May	0.18	717,255	1,200	0.53	0.6
	June	0.14	598,873	1,050	0.49	0.5
	July	0.14	586,403	1,050	0.49	0.5
	August	0.16	650,092	1,200	0.51	0.6
	September	0.18	726,491	1,800	0.53	1.0
	October	0.32	1,103,218	3,000	0.61	1.8
	November	0.41	1,301,353	6,600	0.66	4.4
	December	0.41	1,297,365	1,140	0.66	7.5
D24	January	3.09	2,205,427	15,600	0.98	15.2
	February	2.912	2,149,313	8,100	0.94	7.6
	March	2.61	2,043,625	4,500	0.89	4.0
	April	2.18	1,881,096	3,000	0.81	2.4
	May	1.59	1,622,111	2,400	0.68	1.6
	June	1.28	1,476,224	2,100	0.61	1.3
	July	1.07	1,370,258	1,950	0.55	1.1
	August	0.98	1,323,391	2,100	0.52	1.1
	September	1.00	1,333,703	2,700	0.52	1.4
	October	1.51	1,585,399	4,500	0.66	2.9
	November	2.20	1,889,172	9,900	0.81	8.0
	December	2.81	2,114,340	*N/A*	0.93	*N/A*

[a]Estimates were made by calculating the heat capacity of the monthly-averaged water volume for the past 34 years at flow gauges at Hollinsclough (D4) and Izaak Walton (D24) on the River Dove. Note that in December, at site D24, solar radiation receipt is insufficient to achieve the heat capacity.

upstream quickly render local solar radiation receipt insignificant to Tw variations at that site. Instead, Tw is driven by the cumulative energy advected from upstream. Consequently, as distance downstream increases, shading over longer reaches is required to influence local Tw. Therefore, for all but the first few 100s meters of river, shading has limited impact on the site of planting but can contribute to downstream cooling. For example, at Hollinsclough direct solar radiation would have to be completely intercepted over 0.5 km to change Tw by 1°C at midday in July. At Izaak Walton (where discharge is on average five times greater than at Hollinsclough), the equivalent figure is 1.1 km of shade. It should also be noted that these are likely to be lower bound estimates given our assumptions that no radiation penetrated trees and of maximum possible radiation receipt, under continuous clear sky conditions.

Several studies have measured higher rates of change of Tw (°C/km) for the opposite case when rivers emerge from areas of native vegetation to open pasture. For example, *Rutherford et al*. [1997] find that daily maximum Tw in summer can change by 3–4°C in 600 m for a river in Hamilton, New Zealand (38°S; average width 1.2 m); similarly, *Hopkins* [1971] obtains 3–4°C in 500 m for second-order streams in Wellington, New Zealand (41°S; 1.5–2.0 m wide). Even higher rates of change in maximum Tw of 10°C/km are reported by *Rutherford et al*. [2004] for streams in Western Australia and south-east Queensland (26–35°S; 1.3–3.3 m wide). However, all these field sites are closer to the equator than the River Dove (52°N; average width 6.9 m; range 0.5–11.7 m) so receive more intense solar radiation (equation (3)). Reported discharges of < 30 Ls^{-1} also mean that the volumes of flow being heated are less than those in the Dove, even for summer minima (typically >50 Ls^{-1} at the Hollinsclough gauge).

Tributary influences are a further consideration because they increase the water surface receiving direct solar radiation and input point sources of heat to the main channel. The Dove has little surface drainage and, consequently, tributaries contribute 43% of the cumulative heat whereas in the Manifold, with a dense, dendritic channel network, tributaries provide 88%. As a result, the Dove gains only 36% of the energy that the Manifold accumulates a year, despite the Dove draining a larger catchment. Overall, the significance of a tributary to the thermal regime of a river network depends on the ratio of catchment area to that of the main channel upstream recognizing that groundwater inputs, abstraction, reservoirs, and other factors may further influence Tw.

Shade has greatest effect where water volumes are small and where there is little upstream channel length, such as in headwaters. However, countering this is the fact that headwaters have limited exposure time to solar radiation, limited surface area over which to receive radiation and are strongly influenced by groundwater inputs [*D'Angelo et al*., 1993]. River sources are also more likely to be affected by landscape and microtopographic shade, reducing the relative significance of riparian shade. It is, therefore, likely in the Dove and Manifold that tree shade will have effect over only relatively short reaches of river, supporting the findings of *Chang and Lawler* [2011] for streams in Oregon, USA. In other catchments, wide, shallow streams set in broad floodplains could benefit, provided that the channel is shaded at high solar angles. However, closer to the equator, shadow length is smaller due to high solar angles, reducing the potential significance of riparian shading.

Logistic regression models support these findings. Increased tree cover is expected to be of greatest benefit where α and γ are both relatively high, indicating sensitivity to Ta (the proxy for solar radiation) enabling rivers to reach high Tw. However, the model asymptote (α) increases with distance downstream as exposure time to solar radiation increases, reflecting increased advection of heat with distance downstream, whereas the gradient parameter (γ) decreases as water volumes (thermal inertia) increase. At intermediate distances (5–19 km from source in the Dove), where both parameters are relatively high, riparian shade is likely to be most beneficial for Tw management. Therefore, logistic Ta-Tw regression parameters (α and γ) can help inform site selection for tree planting but this presupposes existence of sufficient Tw and Ta sampling points to detect spatial variations in these metrics [*Johnson et al*., 2014; *Wilby et al*., 2014].

4.4. Other Heat Sources and Future Change

Trees increase long-wave radiation reaching the ground and also modify latent and sensible heat fluxes by altering the microclimate above rivers flowing through riparian woodland [see *Moore et al*., 2005 review]. However, these heat sources are relatively insignificant for much of the time [e.g., *Evans et al*., 1998] and the impact of riparian shade in reducing short-wave radiation more than offsets potential increases in energy from these other sources [*Moore et al*., 2005]. It is unclear whether riparian shade would alter other sources of heat in rivers, such as from precipitation. Although rainfall typically contributes less than 1% of the total energy input to a stream [*Webb and Zhang*, 1997; *Evans et al*., 1998] intense summer storms can produce more rapid rises in Tw than intense solar heating under clear sky conditions [*Wilby et al*., 2015].

To place our estimated shade lengths (0.5–1.1 km) in context, the UKCP09 central estimate of projected change in the warmest day in summer is $+5°C$ by the 2080s under medium emissions [*Murphy et al*., 2009]. Logistic regression models for D4 and D24 predict that the corresponding change in maximum daily Tw would be $+0.7°C$ and $+0.5°C$, respectively. This in turn suggests that less than 1 km of additional riparian shade would be sufficient to offset projected anthropogenic warming to century end. Again, this assumes no radiation penetrates the canopy and that changes in solar radiation may be neglected (despite the possibility of reduced summer mean cloud cover). On the other hand, an outlook of lower river flow volumes in summer implies that the associated changes in Tw (and attendant need for tree planting) are conservative [*Prudhomme et al*., 2012].

The UKCP09 projections suggest substantial increases in sunshine duration and solar radiation, but less downward diffuse radiation [*Tham et al*., 2011]. Further research is needed to establish how these changes might combine in future Tw and hence to ascertain the rivers and reaches that would benefit most from riparian shade management. A more sophisticated approach is needed to interpret the great variability in stream Tw responses to rising global temperatures, including for example recent cooling trends in many rivers of the Pacific continental U.S. [*Arismendi et al*., 2012]. For example, *Kibler et al*. [2013] report that clear felling in one headwater of southwest Oregon resulted in marked cooling of the stream. Similarly, *Janisch et al*. [2013] found Tw response to clear felling in headwaters in western Washington, USA, was small and highly variable between sites. Other works suggests that the relationship between canopy cover and Tw may be moderated by intermittency in surface flow [*Janisch et al*., 2013]. These disparate results underline the importance of local context in shaping energy receipts and hydrological controls of Tw.

4.5. Wider Implications for River Management

The potential benefit of shade is determined by channel characteristics. At the most fundamental level, in the northern hemisphere vegetation should be located on the south bank of rivers to maximize shading of the channel [*Larsen and Larsen*, 1996]. Channels aligned north-south will not be shaded at midday, when the sun is most powerful, except by overhanging vegetation. In order to reduce the radiation receipt of a 10 m wide stream by more than 50% at 52°N latitudes, a tree on the south bank of a river and 5 m from its edge must be at least 12 m tall. Ash requires ~20 years to attain this height and at least 50 years under ideal condition to reach 30 m [*Dobrowolska et al*., 2011]. Recalling that at least 0.5 km of complete shade would be required to cool the Dove by 1°C, riparian buffer zones would have to be several trees deep in order to provide complete shade. In practical terms, it may be challenging to persuade landowners to allow such widespread tree planting, particularly in Europe where the average agricultural land holding is only 0.14 km^2 [*EU Agricultural Census*, 2010]. Therefore, the cooperation of multiple land-owners and a relatively large percentage of their holding would need to be given over to tree cover if this adaptation strategy is to have a discernible impact.

Tree planting to cool rivers may be a more tenable proposition in the UK for major land owners such as the Church of England, Crown Estate, Ministry of Defence, or National Trust. Nonetheless, all planting schemes should recognize the potential detrimental impacts on ecosystems caused by altering the light regime, increasing flood hazard, modifying the geomorphic functioning and local water balance of the river. Enhanced rainfall interception and transpiration along woodland edges could increase local water demand, lessen soil moisture, and reduce recharge, particularly during dry summers [*Harding et al*., 1992]. In addition, some habitats could be fundamentally altered by shade with negative impacts on biomass and ecological communities [*Wood et al*., 2014]. Therefore, patchy shade may be more beneficial to the river ecosystem as a whole, but this implies a longer reach given over to trees to achieve the same predicted cooling.

Increased direct solar radiation penetrating the water column, and warming the body of fish or other organisms may cause more stress than increased Tw, per se. However, the impact of direct radiation on aquatic organisms is rarely considered and Tw monitoring conventionally seeks to minimize this factor in measurements [*Johnson and Wilby*, 2013]. There has also been relatively little consideration of the potential impacts of tree planting on nocturnal Tw [*Wilby et al*., 2014]. Whereas large areas of tree cover are required to alter Tw, individual trees, and patches can still be of biological importance by providing fauna local protection from direct solar radiation or highly localized cool refugia [*Everall et al*., 2012]. More research is needed to assess the specific thermal variables that are of significance to aquatic animals and how these conditions might change in the future under climate change with or without more tree cover [*Orr et al*., 2015b].

5. Conclusions

The thermal regimes of exposed river channels are undoubtedly very different to those under tree cover. However, increased riparian shade is not a panacea for climate change and there will be large areas of river that would be little affected by the addition (or removal) of vegetation because of advected heat from upstream, landscape shade, (cool) groundwater, reservoir releases, and/or snowmelt inputs. In addition, further research is needed into how regional climate change could be manifested directly in Tw (due to plausible combinations of changing Ta, radiation balance, cloud cover, magnitude and frequency of extreme events, and precipitation regime). Potential indirect impacts of climate change on Tw through modified volumes of flow in stream and shifting contributions from surface, subsurface, groundwater, and/or snow/ice melt also merit further investigation.

The topographic indices developed herein could provide means of identifying river reaches that are most sensitive to thermal forcing by the atmosphere, and/or potentially most responsive to active shade management. We show that standardizing direct radiation by upstream catchment area provides a useful proxy for heat accumulation along the profile of a river and hence a basis for estimating riparian buffer lengths needed to achieve a unit reduction in Tw. We show that river reaches dominated by surface water but with relatively small discharges, large width: depth ratios and limited landscape shade benefit most from shading. These zones tend to occur in the midreaches of headwater systems (and are further characterized by relatively large α and γ logistic regression parameters). Channel morphology, river orientation, and the presence of wetland areas, ponds, or artificial structures may also be locally significant considerations. Other factors such as slope, stream order, and percent grassland area are known to affect the net benefit of forest land cover on maximum Tw in nival systems [*Chang and Psaris*, 2013], whereas greater storm sewer pipe lengths and network densities moderate Tw in urban environments [*Sabouri et al*., 2013].

In the case of the River Dove, it is estimated that at least 0.5 km of complete shade would be required to off-set each 1°C rise in Tw. In addition, bankside trees over 12 m tall are needed to shade the river, taking at least 20 years to grow. To implement tree planting on this scale in the UK typically requires coordination of many riparian land-owners and interest groups. Any tree planting would also need to assess potential impacts (positive and negative) on river habitat, hydrology, and geomorphology beyond simply reducing Tw. This research underlines the need for shade management to be considered in a much broader, catchment-wide context, and provides evidence of the scale and time needed to achieve intended thermal benefits for small ($\sim$100 km^2), natural catchments in temperate zones. Further work would be necessary to extend the approach to other catchment types such as urban environments where tree planting could help to manage thermal pollution by runoff from paved surfaces.

Acknowledgements
All LUTEN data are freely available for download from www.luten.org.uk. Other data used, including ArcGIS layers, are available by contacting the authors. We appreciate funding from the Wild Trout Trust and access to sites granted by landowners. Thanks to Julia Toone for assistance in the field and Dapeng Yu for analysing GIS layers.

References

Abesser, C., and P. L. Smedley (2008), Baseline groundwater chemistry: The carbonferous limestone aquifer of the Derbyshire Dome, *Br. Geol. Surv. Open Rep. OR/08/028*, British Geological Survey, Keyworth, U. K.

Arismendi, I., S. L. Johnson, J. B. Dunham, R. Haggerty, and D. Hockman-Wert (2012), The paradox of cooling streams in a warming world: Regional climate trends do not parallel variable local trends in stream temperature in the Pacific continental United States, *Geophys. Res. Lett.*, *39*, L10401, doi:10.1029/2012GL051448.

Bowler, D. E., R. Mant, H. Orr, D. M. Hannah, and A. S. Pullin (2012), What are the effects of wooded riparian zones on stream temperature? *Environ. Evid.*, *1*, doi:10.1186/2047-2382-1-3.

Chang, H. and K. Lawler (2011), Impacts of climate variability and change on water temperature in an urbanizing Oregon basin, in *Proceedings of Symposium H04 IUGG2011: Water Quality Trends and Expected Climate Change Impacts, IAHS Publ.*, edited by N. Peters et al., vol. 348, pp. 123–128, Melbourne, Australia.

Chang, H., and M. Psaris (2013), Local landscape predictors of maximum stream temperature and thermal sensitivity in the Columbia River Basin, USA, *Sci. Total Environ.*, *461–462*, 587–600.

Chapra, S. C., G. J. Pelletier, and H. Tao (2008), *QUAL2K: A Modelling Framework for Simulating River and Stream Quality, version 2.11: Documentation and User's Manual*, Civ. and Environ. Eng. Dep., Tufts Univ., Medford, Mass.

Cole, T. M., and S. A. Wells (2002), CE-QUAL-W2: A two-dimensional, laterally averaged, hydrodynamic and water quality model, version 3.1, *Inst. Rep. EL 03-1*, U.S. Army Corps of Eng., Vicksburg, Miss.

Dallas, H. F., and N. A. Rivers-Moore (2012), Critical thermal maxima of aquatic macroinvertebrates: Towards identifying bioindicators of thermal alteration, *Hydrobiologia*, *679*, 61–76.

D'Angelo, D. J., J. R. Webster, S. V. Gregory, and J. L. Meyer (1993), Transient storage in Appalachian and Cascade mountain streams as related to hydraulic characteristics, *J. N. Am. Benthol. Soc.*, *12*, 223–235.

Davies-Colley, R. J., G. W. Payne, and M. van Elswijk (2000), Microclimate gradients across a forest edge, *N. Z. J. Ecol.*, *24*, 111–121.

Dobrowolska, D., S. Hein, A. Oosterbaan, S. Wagner, J. Clark, and J. P. Skovsgaard (2011), A review of European ash (*Fraxinus excelsior* L.): Implications for silviculture, *Forestry*, *84*, 133–148.

Edmunds, W. M. (1971), Hydrogeochemistry of groundwaters in the Derbyshire Dome with special reference to trace constituents, *Rep. Inst. Geol. Sci. 71/7*, Br. Geol. Surv., Keyworth, U. K.

Environment Agency (2012), *Keeping Rivers Cool: Getting Ready for Climate Change by Creating Riparian Shade*, Bristol, U. K.

EU Agricultural Census (2010). [Available at http://ec.europa.eu/eurostat/statistics-explained/index.php/Agricultural_census_2010_-_main_results, last accessed 29 Sept. 2014]

Evans, E. C., G. McGregor, and G. E. Petts (1998), River energy budgets with special reference to river bed processes, *Hydrol. Processes*, *12*, 575–595.

Everall, N. C., A. Farmer, A. F. Heath, T. E. Jacklin, and R. L. Wilby (2012) Ecological benefits of creating messy rivers, *Area*, *44*, 470–478.

Everall, N. C., M. F. Johnson, R. L. Wilby, and C. J. Bennett (2015), Detecting phenology change in the mayfly *Ephemera danica*: Responses to spatial and temporal water temperature variations, *Ecol. Entomol.*, *40*, 90–105.

FAO (2010), Global Forest Resources Assessment 2010: Main Report, Food and Agriculture Organization of the United Nations, Rome *FAO For. Pap. 163*.

Ficklin, D. L., I. T. Stewart, and E. P. Maurer (2013), Effects of climate change on stream temperature, dissolved oxygen, and sediment concentration in the Sierra Nevada in California, *Water Resour. Res.*, *49*, 2765–2782, doi:10.1002/wrcr.20248.

Ficklin, D. L., B. L. Barnhart, J. H. Knouft, I. T. Stewart, E. P. Maurer, S. L. Letsinger, and G. W. Whittaker (2014), Climate change and stream temperature projections in the Columbia River basin: Habitat implications of spatial variation in hydrologic drivers, *Hydrol. Earth Syst. Sci.*, *18*, 4897–4912.

Forestry Commission (2003), *National Inventory of Woodland and Trees*, Edinburgh, U. K.

Fu, P., and P. M. Rich (2002), A geometric solar radiation model with applications in agriculture and forestry, *Comput. Electron. Agric.*, *37*, 25–35.

Greenberg, J. A., E. L. Hestir, D. Riano, G. J. Scheer, and S. L. Ustin (2012), Using LIDAR data analysis to estimate changes in insolation under large-scale riparian deforestation, *J. Am. Water Resour. Assoc.*, *48*, 939–948.

Hannah, D. M., I. A. Malcolm, C. Soulsby, and A. F. Youngson (2008), A comparison of forest and moorland stream microclimate, heat exchanges and thermal dynamics, *Hydrol. Processes*, *22*, 919–940.

Harding, R. J., R. L. Hall, C. Neal, J. M. Roberts, P. T. W. Rosier, and D. G. Kinniburgh (1992), Hydrological implications of broadleaf woodlands: Implications for water use and water quality, *Proj. Rep. 115/03/ST*, Natl. Rivers Auth., Bristol, U. K.

Hopkins, C. L. (1971) The annual temperature regime of a small stream in New Zealand, *Hydrobiologia*, *37*, 397–408.

Isaak, D. J., C. H. Luce, B. E. Rieman, D. E. Nagal, E. E. Paterson, D. L. Horan, S. Parkes, and G. L. Chandler (2010), Effects of climate change and wildfire on stream temperatures and salmonid thermal habitat in a mountain river network, *Ecol. Appl.*, *20*, 1350–1371.

Janisch, J. E., S. M. Wondzell, and W. J. Ehinger (2013), Headwater stream temperature: Interpreting response after logging, with and without riparian buffers, Washington, USA, *For. Ecol. Manage.*, *270*, 302–313.

Johnson, S. L. (2003), Stream temperature: Scaling of observations and issues for modelling, *Hydrol. Processes*, *17*, 497–499.

Johnson, M. F. and R. L. Wilby (2013), Shield or not to shield: Effects of solar radiation on water temperature sensor accuracy, *Water*, *5*, 1622–1637.

Johnson, M. F., R. L. Wilby, and J. A. Toone (2014), Inferring air-water temperature relationships from river and catchment properties, *Hydrol. Processes*, *28*, 2912–2928.

Kelleher, C., T. Wagener, M. Gooseff, B. McGlynn, K. McGuire, and L. Marshall (2012), Investigating controls on the thermal sensitivity of Pennsylvania streams, *Hydrol. Processes*, *26*, 771–785.

Kibler, K. M., A. Skaugset, L. M. Ganio, and M. M. Huso (2013), Effect of contemporary forest harvesting practices on headwater stream temperatures: Initial response of the Hinkle Creek catchment, Pacific Northwest, USA, *For. Ecol. Manage.*, *310*, 680–691.

Larsen, L. L. and S. L. Larsen (1996), Riparian shade and stream temperature: A perspective, *Rangelands*, *18*, 149–152.

Mantua, N., I. Tohver, and A. Hamlet (2010), Climate change impacts on streamflow extremes and summertime stream temperature and their possible consequences for freshwater salmon habitat in Washington State, *Clim. Change*, *102*, 187–223.

Martins, E. G., S. G. Hinch, D. A. Patterson, M. J. Hague, S. J. Cooke, K. M. Miller, M. F. Lapointe, K. K. English, and A. P. Farrell (2011), Effects of river temperature and climate warming on stock-specific survival of adult migrating Fraser River sockeye salmon (*Oncorhynchus nerka*), *Global Change Biol.*, *17*, 99–114.

Mohensi, O., H. G. Stefan, and T. R. Erickson (1998), A nonlinear regression model for weekly stream temperatures, *Water Resour. Research*, *34*, 2685–2692.

Moore, R. D., D. L. Spittlehouse, and A. Story (2005), Riparian microclimate and stream temperature response to forest harvesting: A review. *J. Am. Water Resour. Assoc.*, *41*, 813–834.

Murphy, J. M., et al. (2009), *UK Climate Projections Science Report: Climate Change Projections*, Met Off. Hadley Cent., Exeter, U. K.

Nisbet, T., M. Silgram, N. Shah, K. Morrow, and S. Broadmeadow (2011), Woodland for Water: Woodland measures for meeting Water Framework Directive objectives, *For. Res. Monogr. 4*, For. Res., Surrey, U. K.

NOAA (2014). [Available at http://www.esrl.noaa.gov/gmd/grad/solcalc/calcdetails.html, last accessed 30 Sept 2014.]

Null, S. E., J. H. Viers, M. L. Deas, S. K. Tanaka, and J. F. Mount (2013), Stream temperature sensitivity to climate warming in California's Sierra Nevada: Impacts to coldwater habitat, *Clim. Change*, *116*, 149–170.

Orr, H. G., et al. (2015a), Detecting changing river temperatures in England and Wales. *Hydrol. Processes*, *29*, 752–766.

Orr, H. G., M. F. Johnson, R. L. Wilby, T. Hatton-Ellis, and S. Broadmeadow (2015b), What else do managers need to know about warming rivers? *WIRES Water*, *2*, 55–64.

Osborne, L. L., and D. A. Kovacic (1993), Riparian vegetated buffer strips in water-quality restoration and stream management. *Freshwater Biol.*, *29*, 243–258.

Prudhomme, C., A. Young, G. Watts, T. Haxton, S. Crook, J. Williamson, H. Davies, S. Dadson, and S. Allen (2012), The drying up of Britain? A national estimate of changes in seasonal river flows from 11 Regional Climate Model simulations, *Hydrol. Processes*, *26*, 1115–1118.

Richardson, J. S., and S. Béraud (2014), Effects of riparian forest harvest on streams: A meta-analysis, *J. Appl. Ecol.*, *51*, 1712–1721.

Rutherford, J. C., S. Blackett, C. Blackett, L. Saito, and R. J. Davies-Colley (1997), Predicting the effects of shade on water temperature in small streams, *N. Z. J. Mar. Freshwater Res.*, *31*, 707–721.

Rutherford, J. C., N. A. Marsh, P. M. Davies, and S. E. Bunn (2004) Effects of patchy shade on stream water temperature: How quickly do small streams heat and cool?, *Mar. Freshwater Res.*, *55*, 737–748.

Sabouri, F., B. Gharabaghi, A. A. Mahboubi, and E. A. McBean (2013), Impervious surfaces and sewer pipe effects on stormwater runoff temperature, *J. Hydrol.*, *502*, 10–17.

Story, A., R. D. Moore, and J. S. Macdonald (2003), Stream temperatures in two shaded reaches below cutblocks and logging roads: Downstream cooling linked to subsurface hydrology, *Can. J. For. Res.*, *33*, 1383–1396.

Sweeney, B. W., and J. D. Newbold (2014), Streamside forest buffer width needed to protect stream water quality, habitat, ad organisms: A literature review, *J. Am. Water Resour. Assoc.*, *50*, 560–584.

Thackeray, S. J., et al. (2010), Trophic level asynchrony in rates of phonological change for marine, freshwater and terrestrial environments, *Global Change Biol.*, *16*, 3304–3313.

Tham, Y., T. Muneer, G. J. Levermore, and D. Chow (2011), An examination of UKCIP02 and UKCP09 solar radiation data sets for the UK climate related to their use in building design, *Build. Serv. Eng. Res. Technol.*, *32*, 207–228.

Toone, J. A., R. L. Wilby, and S. Rice (2011), Surface-water temperature variations and river corridor properties, in *Water Quality: Current Trends and Expected Climate Change Impacts*, edited by N. Peters et al., vol. 348, pp. 129–134. IAHS Publ.

van Vleit, M. T. H., F. Ludwig, J. J. G. Zwolsman, G. P. Weedon, and P. Kabat (2011), Global river temperatures and sensitivity to atmospheric warming and changes in river flow, *Water Resour. Res.*, *47*, W02544, doi:10.1029/2010WR009198.

Webb, B. W., and Y. Zhang (1997), Spatial and seasonal variability in the components of the river heat budget, *Hydrol. Processes*, *11*, 79–101.

Wilby, R. L., et al. (2010), Evidence needed to manage freshwater ecosystems in a changing climate: Turning adaptation principles into practice, *Sci. Total Environ.*, *408*, 4150–4164.

Wilby, R. L., M. F. Johnson, and J. A. Toone (2012), The Loughborough University TEmperature Network (LUTEN): Rationale and analysis of stream temperature variations, in *Proceedings of Earth Systems Engineering 2012: Systems Engineering for Sustainable Adaptation to Global Change*, Centre for Earth Systems Engineering Research, Newcastle, U. K.

Wilby, R. L., M. F. Johnson, and J. A. Toone (2014), Nocturnal river water temperatures: Spatial and temporal variations, *Sci. Total Environ.*, *482–483*, 157–173.

Wilby, R. L., M. F. Johnson and J. A. Toone (2015), Storm induced thermal shockwaves in an upland river, *Weather*, *70*, 92–100.

Wood, K. A., R. A. Stillman, R. T. Clarke, F. Daunt, and M. T. O'Hare (2014), Understanding plant community response to combinations of biotic and abiotic factors in different phases of plant growth cycle, *PLOS One*, *7*, e49824.